EXERGETIC EFFICIENCY OF THE EJECTOR OPERATING ACROSS AMBIENT TEMPERATURE IN A COMBINED POWER AND EJECTOR-REFRIGERATION CYCLE

Hossein Akbari[1], Mikhail V. Sorin[2]*

[1]Mechanical Engineering Department, Université de Sherbrooke, Sherbrooke, QC, J1K 2R1, Canada
Hossein.Akbari@USherbrooke.ca

[2]Mechanical Engineering Department, Université de Sherbrooke, Sherbrooke, QC, J1K 2R1, Canada
Mikhail.V.Sorin@USherbrooke.ca

* Corresponding Author

ABSTRACT

Individual interpretation of the exergy produced and exergy consumed in a device operating below and across an ambient temperature results in different exergy efficiency definitions. This paper compares Grassmann and transiting exergy efficiency definitions for an ejector operating within a combined power and ejector refrigeration cycle. The behavior of exergy metrics such as exergy produced, exergy consumed and exergy efficiency of the ejector for different operating conditions, i.e. primary flow, secondary flow, and condenser pressures, are evaluated. The results show that the exergy produced metric reflects the technical purpose of the ejector while increasing with the entrainment ratio and the pressure lift known as the two most important ejector's operating parameters. As a result, the transiting efficiency provides a logical picture of the ejector behavior for different operating conditions. It is also shown that the Grassmann exergy efficiency cannot be an appropriate criterion to evaluate the exergy performance for the ejector operating across ambient temperature.

1. INTRODUCTION

Exergy analysis has become a standard method for the assessment and optimization of thermodynamic systems and their components since the 1960s. For given operating conditions at the inlet and outlet of a component, the exergy transfer, the exergy losses and thus the exergetic performance of the component should be clearly evaluated. However, an extensive literature review reveals that exergetic efficiency is often subject to individual interpretations which leads to several exergy efficiency definitions such as the input-output efficiency (Grassmann, 1950), the consumed-produced efficiency (Brodyansky *et al.*, 1994) and fuel-product efficiency (Tsatsaronis, 1993; Bejan *et al.*, 1996). The shortcomings of different definitions have been well documented (Tsatsaronis, 1993; Brodyansky *et al.*, 1994; Bejan *et al.*, 1996; Marmolejo-Correa and Gundersen, 2012; Sorin and Khennich, 2018). Marmolejo-Correa and Gundersen (2012) provided an extensive discussion regarding the different exergetic efficiencies. They stated that an appropriate exergy efficiency terminology must provide two advantages: the unambiguous definitions of exergy production and consumption, and the ability to properly describe the exergetic effectiveness of a device. They showed that the terminology introduced by Brodyansky *et al.* (1994) is the only expression that can be explicitly used for all processes under different operating conditions. The other proposed definitions failed to express the exergetic performance of a component where the process occurs in sub- or cross- ambient conditions. Brodyansky *et al.* (1994) presented a systematic methodology to calculate the exergetic efficiency based on the transiting exergy (i.e. unaffected part of the thermomechanical exergy entering and leaving the component). Using the transiting exergy definition provides the ability to systematically evaluate the exergy produced and exergy consumed in a process without leaving any room for individual interpretations.

The main objective of this paper is to study the ability of two well-known exergetic efficiencies, transiting and Grassmann, to describe the exergetic effectiveness of the ejector under different operating conditions (primary flow, secondary flow, and outlet pressures).

2. SYSTEM DESCRIPTION

The schematic diagram of the proposed combined ORC and ejector-driven refrigeration cycle is illustrated in Figure 1 (Habibzadeh *et al.*, 2013).

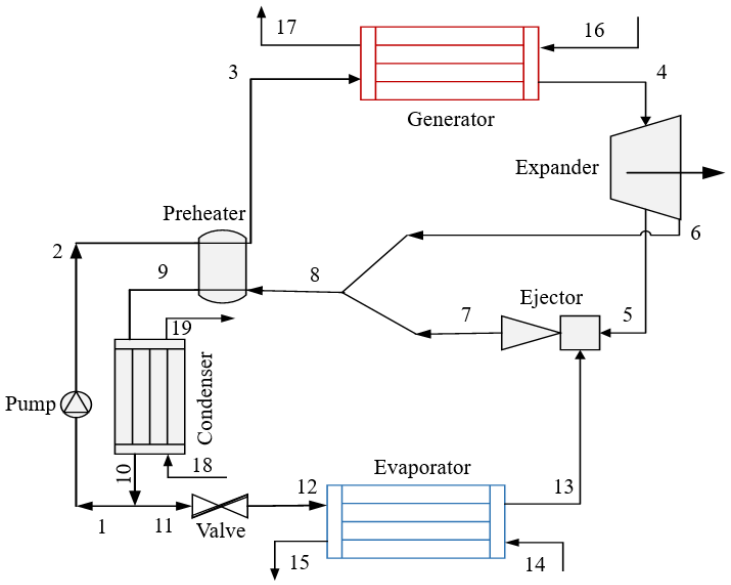

Figure 1: schematic diagram of the proposed combined ORC and ejector refrigeration system

The system is composed of an expander, an ejector, a pump, a throttling valve, and four heat exchangers including generator, condenser, evaporator and preheater. A part of saturated liquid leaving the condenser is pumped to the highest pressure of the cycle. The refrigerant temperature is increased by passing through the preheater before absorbing heat from the high-temperature source in the generator. The high-pressure, high-temperature vapor enters the turbine to generate mechanical power. A fraction of the partially expanded refrigerant at state 5 is withdrawn from the expander and enters the ejector as its motive stream. This flow expands to a very low pressure by passing through the converging-diverging nozzle and entrains the secondary flow from the evaporator into the mixing chamber. Both streams are assumed to be completely mixed together at the end of the mixing chamber. A normal shock (which replaced the oblique shock wave) occurs within the constant-area section, creating a compression effect. Then the mixed stream enters a subsonic diffuser and reaches the condenser pressure. The compressed combined stream leaving the ejector is mixed with the fully expanded refrigerant leaving the expander (state 6) and its temperature is decreased in the preheater. The vapor at state 9 enters the condenser and liquefied by rejecting heat to the cooling water. The saturated liquid at the condenser outlet is divided into two streams. A part of condensed working fluid returns to the pump and the remaining passes an isenthalpic process through the throttling valve and its pressure is decreased before entering the evaporator. The refrigerant produces the required cooling load by absorbing heat from the cooled medium in the evaporator before entering the ejector as the secondary flow.
Conducting energy and exergy investigation in the ejector-based cycles reveals that the ejector is responsible for the one of the most important irreversibility in the cycles (Chen *et al.*, 2017; Eldakamawy *et al.*, 2017; Li. F. *et al.*, 2018) and optimal design of ejector will definitely improve the overall efficiency of the system. The purpose of the ejector is to compress the induced fluid from a lower pressure to a higher pressure. The most important parameters for ejector design are the entrainment ratio, i.e. the ratio of entrained mass flow rate to the primary mass flow rate (Eq. (1)), and the pressure ratio, i.e. the ratio of the evaporator to the condenser pressures (Eq. (2)) (Taleghani *et al.*, 2018).

$$\omega = \frac{\dot{m}_{13}}{\dot{m}_5} \tag{1}$$

$$PR = \frac{P_{13}}{P_7} \tag{2}$$

3. EXERGY EFFICIENCIES IN THE EJECTOR

In this section, two different exergy efficiencies proposed for the ejector will be introduced:

3.1 Input-output (Grassmann) efficiency

This efficiency is defined as the ratio of the exergy of the mixed fluid leaving the ejector to the exergy of primary and secondary fluids entering the ejector. This definition has been used in the majority of papers published in the literature (Ahmadzadeh *et al.*, 2017; Boyaghchi and Asgari, 2017; Zhao *et al.*, 2016). It should be mentioned that in nearly all the papers, the summation of the exergy of fluids entering the ejector assumed as the fuel exergy, i.e. the net resources spent to generate the purpose of using the system (Tsatsaronis, 1993), of the ejector and the outlet exergy as the produced exergy of the ejector. Thus, the input-output efficiency is equivalent to the fuel-product efficiency in this case.

$$\eta_{Gr} = \frac{(\dot{m}_5 + \dot{m}_{13}) \cdot ex_7}{\dot{m}_5 \cdot ex_5 + \dot{m}_{13} \cdot ex_{13}} = \frac{E_7}{E_5 + E_{13}} \tag{3}$$

3.2 Transiting efficiency

Brodynasky et al. (1994) presented a systematic methodology to calculate the exergetic efficiency based on the transit exergy (minimum exergy value that a refrigerant may experience during a process). They presented three possible conditions based on the ambient temperature, T_0:

$$if\ (T_{in} > T_0\ and\ T_{out} > T_0):\ ex^{tr} = ex(T_{min}, P_{min}) \tag{4}$$

$$if\ (T_{in} < T_0\ and\ T_{out} < T_0):\ ex^{tr} = ex(T_{max}, P_{min}) \tag{5}$$

$$if\ (T_{in} > T_0\ and\ T_{out} < T_0)\ OR\ (T_{in} < T_0\ and\ T_{out} > T_0):\ ex^{tr} = ex(T_0, P_{min}) \tag{6}$$

The great advantage of transiting terminology is that it provides clear and systematic definitions of consumed and produced exergies in a process for different conditions while the other definitions encounter a serious problem in sub- or crossing ambient temperature conditions. The exergy consumed, exergy produced and the transiting exergy efficiency of an ejector are (Sorin and Khennich, 2018):

$$\nabla E = \left(\dot{m}_5 \cdot \nabla \mathrm{ex}_p\right) + \left(\dot{m}_{13} \cdot \nabla \mathrm{ex}_s\right) = \dot{m}_5 \cdot \left(ex_p - ex_p^{tr}\right) + \dot{m}_{13} \cdot \left(ex_s - ex_s^{tr}\right) \tag{7}$$

$$\Delta E = \left(\dot{m}_5 \cdot \Delta \mathrm{ex}_p\right) + \left(\dot{m}_{13} \cdot \Delta \mathrm{ex}_s\right) = \dot{m}_5 \cdot \left(ex_7 - ex_p^{tr}\right) + \dot{m}_{13} \cdot \left(ex_7 - ex_s^{tr}\right) \tag{8}$$

$$\eta_{Gr} = \frac{\Delta E}{\nabla E} \tag{9}$$

The exergy-enthalpy and Grassmann diagrams of an ejector where its primary and outlet flows are located in the above ambient conditions while secondary flow crosses the ambient temperature are illustrated in **Figure 2**. According to **Figure 2**a, the first term of exergy consumption (Eq. (7)) represents the decrease of the thermo-mechanical exergy due to the temperature and pressure drops in the expansion process of the primary fluid. The second term of Eq. (7) represents the decrease of the specific thermal exergy of the secondary stream due to the temperature rise from T_{13} to T_0.

The first term of produced exergy (Eq. (8)) is zero, meaning that there is no assignment of the primary flow to the produced exergy (**Figure 2**b). The second term of Eq. (8) constitutes the thermo-mechanical exergy produced by the secondary flow, due to the pressure rise from P_{13} to P_7 and temperature rise from T_0 to T_7. Grassmann diagram (**Figure 2**b) also reveals that the consumed exergy in the ejector is linked to the both primary and secondary flows whilst the produced exergy related solely to the secondary flow.

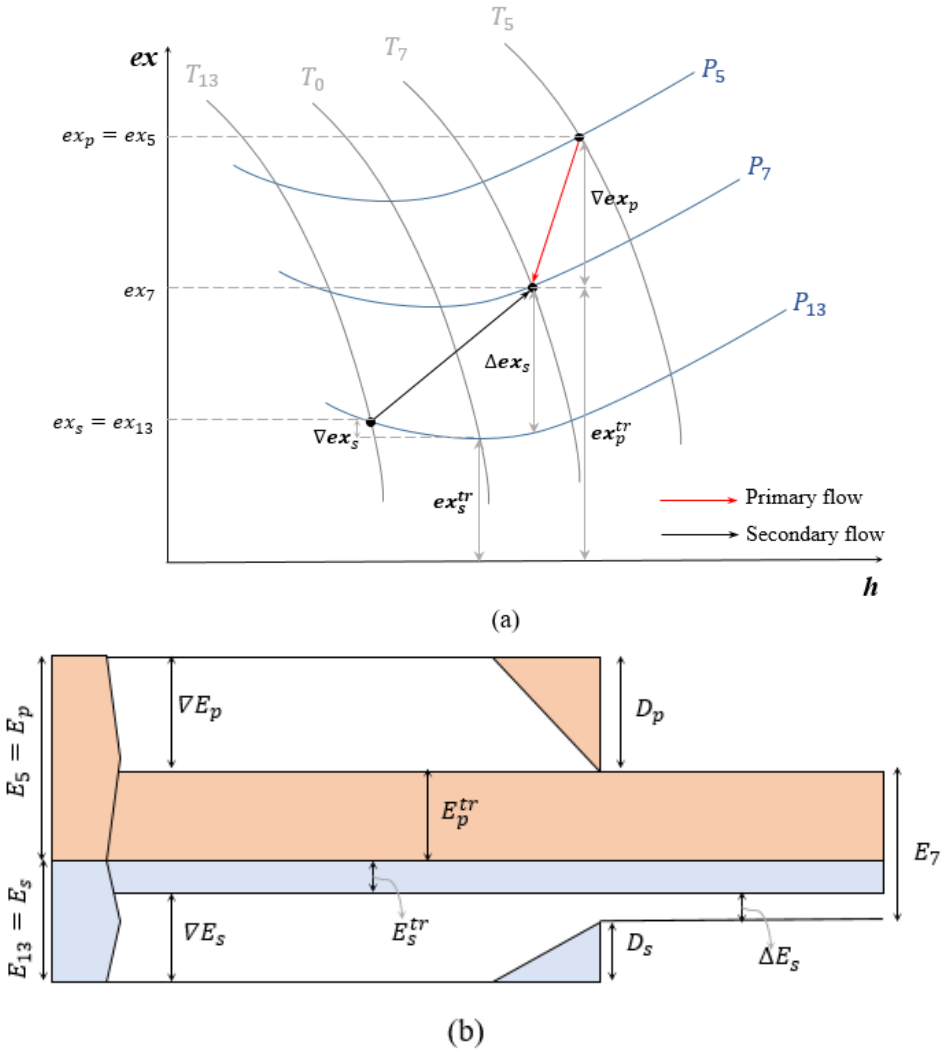

Figure 2: exergy-enthalpy (a) and Grassmann (b) diagrams of an ejector where

$$T_{13} < T_0 \; and \; T_7, T_5 > T_0$$

4. MODELING EQUATIONS AND SOLUTION PROCEDURE

The procedure for the numerical solution of the thermodynamic model of the system and its validation are available in Habibzadeh *et al.* (2013). Dimethyl ether was chosen as the working fluid for the system in this work. The proposed values for modeling the base case scenario are presented in Table 1. It is assumed that the ejector operated at the on-design conditions (critical point) and 1-D thermodynamic modeling of the ejector procedure and its important constant values are available in Eldakamawy *et al.* (2017). The numerical model was performed in MATLAB, and thermodynamic properties of the working fluid were called from CoolProp library.

Table 1: proposed values for the base case scenario

Environment temperature	$T_0 = 298.15 \quad K$
Environment pressure	$P_0 = 101.3 \quad kPa$
Turbine inlet pressure	$P_4 = 2250 \quad kPa$
Expansion ratio of the turbine	$\beta = P_4/P_5 = 2.5$
Extraction ratio	$R = \dot{m}_5/\dot{m}_4 = 0.3$
Turbine isentropic efficiency	$\eta_T = 0.8$
Pump isentropic efficiency	$\eta_P = 0.8$
Heat source inlet temperature	$T_{16} = 393.15 \quad K$
Heat source mass flow rate	$\dot{m}_H = 285.9 \quad kg/s$
Cooling water inlet temperature	$T_{18} = 283.15 \quad K$
Evaporation temperature	$T_{12} = 268.15 \quad K$
Temperature difference	$\Delta T = 5 \quad K$

5. RESULTS AND DISCUSSION

In order to compare the exergetic efficiencies of the ejector, different operating conditions of the ejector will be considered and the effect of the operating conditions of the ejector on the exergetic efficiencies will be investigated.

5.1 Primary flow pressure

The first parameters studied herein is the pressure of the primary flow. Table 2 shows the operating performance of the system for different primary flow pressure while other parameters in Table 1 remained constant. It should be mentioned that the thermal efficiency of the system shown in the second column of the table can be calculated as:

$$\eta_{th} = \frac{\dot{W}_{net} + \dot{Q}_{ev}}{\dot{Q}_{gen}} \tag{10}$$

The table shows that the increase of the primary flow pressure leads to higher secondary mass flow rate and thus the system produces more cooling load (higher thermal efficiency).

Table 2: operating performance of the system for different primary pressure of the ejector

P_5 (kPa)	η_{th} (%)	$\dot{W}_{net}$ (kW)	$\dot{Q}_{ev}$ (kW)	$\dot{Q}_{gen}$ (kW)	ω $(-)$	$\dot{m}_{13}$ (kg/s)
900	19.1	1756	879	14205	0.25238	2.2304
1000	20.6	1714	1129	14180	0.32393	2.8627
1125	22.2	1668	1398	14151	0.40118	3.5454
1285	23.9	1615	1692	14118	0.48557	4.2912
1500	25.9	1554	2018	14078	0.57891	5.1161
↑	↑	↓	↑	↓	↑	↑

The exergy metrics inside the ejector for different primary flow pressure are demonstrated in Table 3. It must be noted that the exergy destruction can be calculated by subtracting the exergy produced from the exergy consumed in a process and is identical for transiting and Grassmann terminologies. Table 3 indicates that the transiting efficiency and Grassmann efficiency have different behaviors regarding primary flow pressure rise. This discrepancy is due to their different produced exergy definitions, i.e. Eqs. (3) and (8). The produced exergy calculated by transiting exergy ($\Delta \dot{E}_s$) focuses on secondary flow (its mass flow rate and the pressure lift), whereas the produced exergy in Grassmann model constitutes

the summation of mass flow rates of both primary and secondary flows and the specific exergy of the outlet. Table 2 and Table 3 show a considerable consistency between secondary flow mass flow rate and the produced exergy, calculated by transiting approach. The mass flow rate and $\Delta\dot{E}_s$ went up 229% and 227%, respectively, by increasing the pressure from 900 to 1500 kPa. The produced exergy calculated by the Grassmann for the highest pressure is only 1.25 times as much as that of the lowest pressure. The increase in transiting produced exergy compensated for the increase in exergy losses and resulted in higher transiting exergy efficiency. On the other hand, the increase of exergy losses overweighs the produced exergy rise in the Grassmann approach and leads to lower Grassmann efficiency.

As was mentioned above, the entrainment ratio and pressure lift are the two most important parameters in ejector design. Table 3 demonstrates that transiting exergy efficiency takes these two parameters into account and can be a reliable criterion for exergy evaluation in the ejector. It should be noted that the pressure lift in Table 3 remained constant.

Table 3: Variations in the exergy metrics for different primary flow pressure of the ejector

P_5 (kPa)	$\Delta\dot{E}_s$ (kW)	$\nabla\dot{E}_s$ (kW)	$\nabla\dot{E}_P$ (kW)	$\eta_{tr,eje}$ (%)	$\eta_{Gr,eje}$ (%)	$\dot{D}$ (kW)	$\dot{E}_5$ (kW)	$\dot{E}_{13}$ (kW)	$\dot{E}_7$ (kW)
900	81.27	5.42	338.99	23.6	76.6	263.14	1025.6	97.44	859.9
1000	104.02	6.95	390.9	26.1	75.6	293.83	1076.6	125.06	907.9
1125	128.52	8.61	448.72	28.1	74.5	328.81	1133.7	154.89	959.8
1285	155.28	10.42	514.02	29.6	73.4	369.16	1198.4	187.47	1016.7
1500	184.89	12.42	589.1	30.7	72.2	416.63	1273.1	223.51	1080
↑	↑	↑	↑	↑	↓	↑	↑	↑	↑

5.2 Secondary flow pressure

Evaporator pressure or secondary flow pressure effects on the performance of the system and exergy metrics are given in Table 4. The increase in the entrainment ratio of the ejector leads to higher both exergetic efficiencies even though the pressure ratio drops. It should be noted that due to neglecting transiting exergy flow from the numerator and denominator of the efficiency definition, the transiting terminology always results in lower efficiency value compared to the Grassmann definition.

Table 4: Variations in the exergy and performance metrics and for different secondary flow pressure of the ejector

P_{13} (kPa)	$\Delta\dot{E}_s$ (kW)	$\nabla\dot{E}_s$ (kW)	$\nabla\dot{E}_P$ (kW)	$\eta_{tr,eje}$ (%)	$\eta_{Gr,eje}$ (%)	$\dot{D}$ (kW)	ω $(-)$	PR $(-)$	η_{th} (%)
164.8	14.28	1.019	321.53	4.43	70.17	308.27	0.0299	2.65	13.7
192.2	51.61	2.559	331.16	15.42	73.49	283.11	0.1297	2.28	16.1
223.0	81.27	5.42	338.99	23.6	76.57	263.14	0.2524	1.96	19.1
257.5	102.34	6.622	345.28	29.08	78.92	249.56	0.4086	1.70	23.0
295.8	112.69	7.197	350.24	31.53	81.69	244.75	0.6165	1.48	28.2
↑	↑	↑	↑	↑	↑	↓	↑	↓	↑

5.3 Condenser pressure

The comparison of the exergetic efficiencies of a fixed-geometry ejector was made by Taslimi *et al.* (2018). In the case of fixed-geometry where the condenser pressure plays a key role in the ejector performance, they showed that the Grassmann exergy efficiency is not a proper criterion for exergy efficiency assessment. The exergetic metrics for different backpressure of the ejector where its geometry is not fixed are provided in Table 5.

Table 5: Variations in the exergy and performance metrics and for different backpressure of the ejector

P_7	$\Delta\dot{E}_s$	$\nabla\dot{E}_s$	$\nabla\dot{E}_P$	$\eta_{tr,eje}$	$\eta_{Gr,eje}$	$\dot{D}$	ω	PR	η_{th}	$\dot{E}_7$
(kPa)	(kW)	(kW)	(kW)	(%)	(%)	(kW)	$(-)$	$(-)$	(%)	(kW)
410.9	104.8	7.8	372.4	27.6	76.4	275.3	0.363	1.84	22.1	890.5
437.5	81.3	5.4	339.0	23.6	76.6	263.1	0.252	1.96	19.1	859.9
465.3	56.1	3.4	305.2	18.2	76.8	252.5	0.158	2.09	16.6	834.1
494.5	29.6	1.6	271.0	10.9	77.0	243.1	0.076	2.21	14.3	811.9
↑	↓	↓	↓	↓	↑	↓	↓	↑	↓	↓

Table 5 indicates an inconsistency between the Grassmann and transiting exergy efficiencies. However, the exergy produced and exergy destruction calculated by both approaches decreased. The Grassmann efficiency marginally increased from 76.4% to 77% while the transiting exergy efficiency significantly declined by around 60%, when the ejector's backpressure increased from 410 to 490 kPa. It means that the significant decrease in the transiting produced exergy overweighed the exergy destruction and resulted in remarkable lower transiting exergy efficiency. While the exergy destruction decrease dominated the slight decrease in $\dot{E}_7$ and leaded to a marginal increase in Grassmann efficiency. It should be noted in Table 3, where the pressure lift remained constant, the transiting produced exergy and the entrainment ratio increased with the same rate, while in Table 5, where the pressure lift increased, the rates of transiting produced exergy and entrainment ratio changes were significantly different. Thus, the transiting efficiency can provide a logical picture of the performance of the ejector regarding the entrainment ratio and the pressure lift which reflect the technical purpose of the ejector.

6. CONCLUSIONS

The transiting approach establishes a logical link between the produced exergy and the two important ejector parameters, i.e. entrainment ratio and pressure lift. As a result, the ejector exergy efficiency defined by transiting definitions is consistent with the ejector exergetic effectiveness for different working conditions, while Grassmann efficiency behaves in the opposite way and does not reflect the technical performance of an ejector.

ACKNOWLEDGMENT

This project is a part of the Collaborative Research and Development (CRD) Grants Program at "Université de Sherbrooke". The authors acknowledge the support of the Natural Sciences and Engineering Research Council of Canada, Hydro-Québec, Rio Tinto, Alcan and Canmet ENERGY Research Center of Natural Resources Canada (RDCPJ451917-13).

NOMENCLATURE

E	Exergy	(kW)
D	Exergy destruction	(kW)
P	Pressure	(kPa)
PR	Pressure ratio	(-)
Q	Thermal power	(kW)
T	Temperature	(K)
W	power	(kW)
ex	specific exergy	(kJ/kg)
m	mass flow rate	(kg/sec)

Subscript

Gr	Grassmann
H	Heat source
P	Pump
T	Turbine
ev	Evaporator
gen	Generator
p	primary
s	secondary
tr	transiting
th	thermal

Greek symbols

η	Efficiency
ω	Entrainment ratio
∇	Consumption
Δ	Production

REFERENCES

Ahmadzadeh A, Salimpour MR, Sedaghat A., 2017, Analyse thermique et exergoéconomique d'un nouveau système solaire combinant production d'électricité et de froid par éjecteur. *Int J Refrig*; vol. 83, p. 143–156.

Bejan A, Tsatsaronis G, Moran M., 1996, *Thermal design and optimization.* John Wiley, New York, NY, USA.

Boyaghchi FA, Asgari S., 2017, A comparative study on exergetic, exergoeconomic and exergoenvironmental assessments of two internal auto-cascade refrigeration cycles. *Appl Therm Eng*; vol. 122, p. 723–737.

Brodyansky VM, Sorin M V., Goff TJA Le., 1994, *The Efficiency of Industrial Processes: Energy Analysis and Optimization*. Elsevier Science Ltd, Amsterdam, Netherlands.

Chen J, Zhu K, Huang Y, Chen Y, Luo X., 2017, Evaluation of the ejector refrigeration system with environmentally friendly working fluids from energy, conventional exergy and advanced exergy perspectives. *Energy Convers Manag*, vol. 148, p. 1208–1224.

Eldakamawy MH, Sorin M V, Brouillette M., 2017, Energy and exergy investigation of ejector Étude de l ' énergie et de l ' exergie des systèmes frigorifiques à éjecteur fonctionnant avec des frigorigènes rétrogrades. *Int J Refrig*, vol. 78, p. 176–192.

Grassmann P., 1950, Zur allgemeinen Definition des Wirkungsgrades. *Chemie Ing Tech – CIT*, vol. 22, p.77–80.

Habibzadeh A, Rashidi MM, Galanis N., 2013, Analysis of a combined power and ejector-refrigeration cycle using low temperature heat. *Energy Convers Manag*, vol. 65, p. 381–391.
Li F, Chang Z, Li X, Tian Q., 2018, Energy and exergy analyses of a solar-driven ejector-cascade heat pump cycle. *Energy*, vol. 165, p. 419–431.

Marmolejo-Correa D, Gundersen T., 2012, A comparison of exergy efficiency definitions with focus on low temperature processes. *Energy* , vol. 44, p. 477–489.

Sorin M, Khennich M., 2018, Exergy Flows Inside Expansion and Compression Devices Operating below and across Ambient Temperature. Energy Syst. Environ., vol. 2, InTech, p. 64.

Taleghani ST, Sorin M, Poncet S., 2018, Exergy performance of a transcritical CO_2 two- phase ejector. *31ST Int. Conf. Effic. COST, Optim. Simul. Environ. IMPACT ENERGY Syst., Guimarães, Portugal*.

Tsatsaronis G., 1993, Thermoeconomic analysis and optimization of energy systems. *Prog Energy Combust Sci*, vol. 19, p.227–257.

Zhao Y, Wang J, Cao L, Wang Y., 2016, Comprehensive analysis and parametric optimization of a CCP (combined cooling and power) system driven by geothermal source. *Energy*; vol. 97, p. 470–487.